This is a pre-print version of:
Frediani, A., Cipolla, V., Oliviero, F. et al. A new ultralight amphibious PrandtlPlane: preliminary CFD design of the hull. Aerotec. Missili Spaz. 92, 77 - 86 (2013). https://doi.org/10.1007/BF03404665

A new ultralight amphibious PrandtlPlane: preliminary CFD design of the hull *

A. Frediani[a], V. Cipolla[b], F. Oliviero [a], M. Lucchesi, T. Lippi, S. Luci

[a]Università di Pisa, Dipartimento di Ingegneria Civile e Industriale

[b]SkyBox Engineering S.r.l., Pisa

Abstract

This paper describes the preliminary CFD analyses of a ultralight amphibious PrandtlPlane, performed in order to the define the hull configurations to be studied in a subsequent towing tank test campaign. By taking the Italian regulations on ultralight aircraft into account, the effects of the main design parameters on take-off manoeuvre are studied and two hull configurations are defined. Finally, the achieved results are discussed in order to define the scale factor of towing tank test models.

1. Introduction

Figure 1. Artistic view (top) and full-scale prototype (bottom) of the ultralight amphibious PrandtlPlane

The present paper shows some results about the preliminary design of the hull of a ultralight amphibious PrandtlPlane [1], shown in Figure 1. Such innovative aircraft has been the object of a research project called IDINTOS, coordinated by the Aerospace Section of the Civil and Industrial Engineering Department of Pisa and ended in August 2013 with the manufacturing of a full-scale prototype (Figure 1).

The PrandtlPlane configuration derives from the "best wing system" concept by Ludwig Prandtl, who in 1924 demonstrated that a box-wing system, under proper conditions, provides the minimum induced drag for given lift and wingspan [2]. When applied to ultralight aircraft, the PrandtlPlane layout can improve flight safety without reducing aircraft performance [3].

The research here presented is focused on take-off run of the amphibious PrandtlPlane, which has been studied by means of the CFD code STAR-CCM+ by CD-Adapco. It is worth of notice that such analyses have been carried out in order to prepare a towing tank test campaign, using CFD results to define some hull configurations and their performance, with the aim of reducing the uncertainties of the experimental phase.

2. Seaplanes characteristics

Amphibious aircraft are able to operate on both water and land, being provided with retractable landing gears. As Figure 2 shows, the floating fuselage here considered consists of a hull with a keel and two hard chines, which define a V-shaped cross section. A fundamental element of a seaplane hull is a sharp discontinuity on the bottom surface, consisting of a transversal step which separates the hull in two parts, called "forebody" and "afterbody". Figure 2 illustrates the main geometric parameters which define

*Results shown in this paper have been achieved during the research project "IDINTOS", funded by Tuscany Region (Italy) in 2011

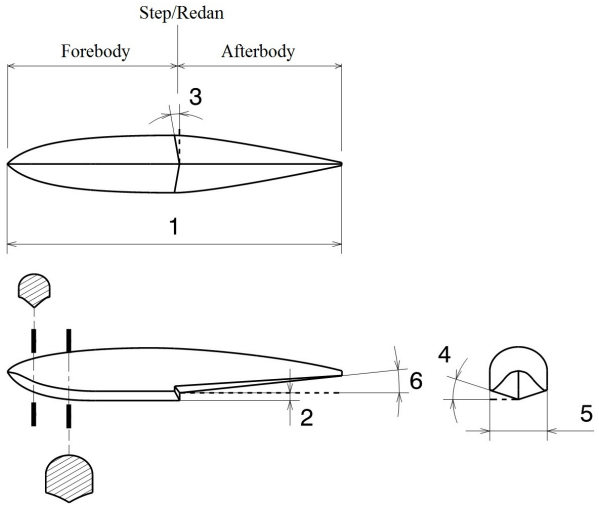

Figure 2. Design parameters of a hull: length (1), step height (2), step planform angle (3), dead-rise angle (4), maximum beam (5), angle of afterbody keel (6)

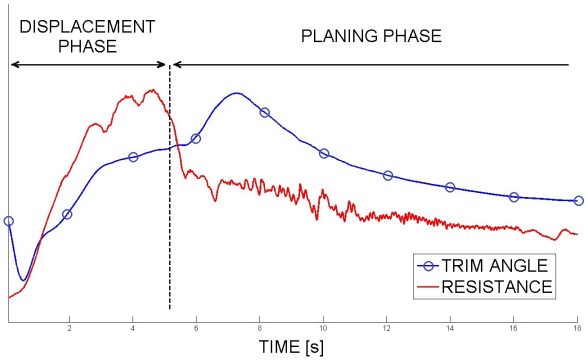

Figure 3. Example of resistance and pitch angle during take-off run

the shape of a hull.

During the take-off run of a seaplane, water drag, hereafter called "resistance", and pitch angle vary as shown in Figure 3. Two phase can be identified:

1. Displacement phase: after the engine ignition, the pitch angle reaches its minimum as a consequence of the nose-down moment introduced by thrust. The hull accelerates and resistance increases with speed, while the water flowing under the hull separates at step's edge. As speed rises, the hydrodynamic pressure increases the vertical displacement and the separated region behind the step is gradually filled by air coming from hull's sides. The wetted region moves backwards, the contact area gets smaller and the grow rate of resistance decreases.

2. Planing phase: the previous phase ends when resistance reaches a maximum ("hump") and, after that, drops rapidly because of the reduction of wetted surface. In this phase, the hull "sits" on the step with a smaller pitch angle and its weight is progressively sustained by hydrodynamic lift instead of buoyancy. The lower resistance allows the seaplane to further accelerate and the aerodynamic effectiveness of control surface is increased, allowing the pilot to complete the take-off manoeuvre.

During both phases, the hard chines make the water flow separate from hull's sides, reducing water resistance, and the V-shaped section provides lateral stability. The dead-rise angle is usually smaller at step, in order to reduce the resistance during planing, and it is bigger at bow, to improve the ability of the hull to cut through waves in rough water.

One of the main issues of hulls' dynamics is a motion instability called "porpoising" [4], which consists in oscillations of both pitch angle and vertical displacement, whose amplitude can be constant or increase, even in smooth water. This phenomenon causes resistance increase, reduction of aircraft's controllability and may lead to catastrophic failure.

2.1. Planing-tail hulls

In the present paper "planing-tail" hulls have been considered as well. This configuration differs from the "conventional" one for the following aspects: the centre of gravity (CG hereafter) is positioned between the step and the hull's stern, the afterbody is much longer, the step is deeper and the angle of the afterbody keel is smaller. The distinctive feature of a planing-tail hull lies in its behaviour during the planing phase: contrary to a conventional configuration, where the contact with water occurs at step, there is a second contact area at stern, as shown in Figure 4.

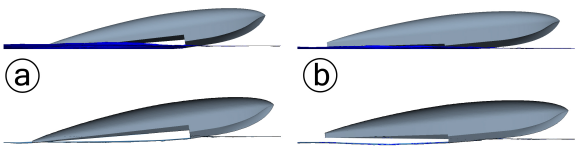

Figure 4. Planing-tail (a) and conventional (b) configurations

This is a pre-print version of:
Frediani, A., Cipolla, V., Oliviero, F. et al. A new ultralight amphibious PrandtlPlane: preliminary CFD design of the hull. Aerotec. Missili Spaz. 92, 77 - 86 (2013). https://doi.org/10.1007/BF03404665

Past NACA studies have shown important advantages of planing-tail hulls, such as a reduction in resistance during planing phase and a wider range of pitch angle and speed conditions free from porpoising [5], [6], [7].

3. Aircraft design

The starting point for the design of a ultralight amphibian is given by a set of requirements defined by national or international regulations. For the IDINTOS project, the Italian regulations on ultralight aircraft has been taken into account [8], [9].

Regulations' requirements must be fulfilled for the whole longitudinal range of CG, therefore weight distribution and load conditions have been established, as reported in Section 3.1.

3.1. Weight distribution

A preliminary estimation of weights and CGs is based on a simplified model, which takes fuselage, wing system, pilots, fuel tanks (main + reserve), landing gears, engine, propellers, avionics, ballistic parachute, batteries and ballast into account.

Table 1 shows the values of weight and CG position, given as the distance from bow, in the most significant operative conditions, for the aircraft configuration resulting from the preliminary design [10].

Table 1
Weights and CGs

Condition	Pilots	Fuel [kg]	Ballast [kg]	Weight [kg]	X_{CG} [mm]
Empty	0	0	0	330	3852
MTOW	2	17	0	495	3543
CG min	2	65	0	584 [2]	3498
CG max	1	15	12.5	429	3611

3.2. Amphibious PrandtlPlane configuration

As shown in Figure 5, the amphibian has 2 ducted propellers, auxiliary floats (which can be used as fuel tanks) and control surfaces on both wings. In addition, the aircraft is provided with a retractable landing gear, located between the cabin and the step section, a nose wheel and a ballistic parachute.

The configuration shown has been obtained taking the following aspects into account:

- requirements related to weights, aerodynamics (e.g.: stall), flight mechanics and safety, according to Italian regulations;

[2]Maximum design weight

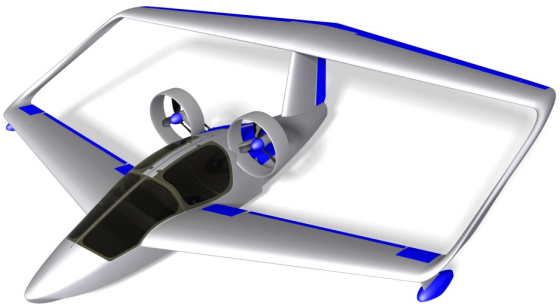

Figure 5. CAD model of the ultralight amphibious PrandtlPlane

- equilibrium and stability in water during take-off manoeuvre;
- buoyancy in the case of failure of 2 watertight compartments;
- low level of accelerations during emergency sea landing;
- ergonomics of interiors and pilots visibility (Figure 6).

In the following of the paper, CFD analyses of take-off run and emergency sea landing manoeuvres are briefly described.

Figure 6. Visibility and ergonomic tests on a full-scale maquette (ISIA, Florence)

4. CFD analysis of take-off run

The CFD analysis of take-off run has been performed by means of the software STAR-CCM+ (ver-

This is a pre-print version of:
Frediani, A., Cipolla, V., Oliviero, F. et al. A new ultralight amphibious PrandtlPlane: preliminary CFD design of the hull. Aerotec. Missili Spaz. 92, 77 - 86 (2013). https://doi.org/10.1007/BF03404665

sions 5 and 6), which has been used to simulate the manoeuvre from the initial 0 speed condition to take-off. The hull has been modelled in STAR-CCM+ to calculate forces and moments applied by both air and water on it, while external forces due to wing system and propellers have been introduced by means of simplified formulas, depending on speed and pitch angle.

In particular, the CFD analysis has been focused on the effects of hull's design parameters on take-off characteristics, such as resistance, pitch angle, speed and stability.

4.1. CFD models and solvers

The CFD code has been used to integrate the equations of motion and to provide the values of resistance, lift, moments, accelerations, vertical displacement, pitch angle, speed and covered distance as functions of time.

The *Volume Of Fluid*(VOF) model has been used to simulate the free surface, dividing water and air phases. This interface is modelled as an equivalent fluid, whose physical properties depend on those ones of constituent phases and volume fraction of each of them, which is defined as follows:

$$\alpha_{\mathbf{i}} = \mathbf{V_i}/\mathbf{V}, \tag{1}$$

where V_i is the volume of the i$^{\text{th}}$ phase and V is the total volume.

The multiphase flow is solved with incompressible RANS equations, with both air and water densities assumed as constant. The turbulence model chosen is the *Realizable Two-Layer* κ-ϵ; the boundary layer is modelled by means of the *Two Layer All y+* wall treatment.

The hull is modelled as a rigid body with pitch rotation, vertical and horizontal displacement as degrees of freedom. The domain mesh rotates and moves together with the hull.

Aerodynamic lift L and pitching moment m are introduced through the following expressions:

$$\begin{aligned}\mathbf{L} = \tfrac{\mathbf{1}}{\mathbf{2}} \cdot \boldsymbol{\rho_0} \cdot \mathbf{S} \cdot \mathbf{V^2} \cdot \Big[\mathbf{C_{L0}} + \\ + \mathbf{C_{L\alpha}} \cdot \Big(\alpha - \arctan \tfrac{\mathbf{v_z}}{\mathbf{v_x}}\Big)\Big]\end{aligned} \tag{2}$$

$$\begin{aligned}\mathbf{m} = \tfrac{\mathbf{1}}{\mathbf{2}} \cdot \boldsymbol{\rho_0} \cdot \mathbf{S} \cdot \mathbf{c} \cdot \mathbf{V^2} \cdot \Big[\mathbf{C_{m0}} + \\ + \mathbf{C_{m\alpha}} \cdot \Big(\alpha - \arctan \tfrac{\mathbf{v_z}}{\mathbf{v_x}}\Big)\Big]\end{aligned} \tag{3}$$

where ρ_0 is the air density at sea level, S is the wing system surface, c is the mean aerodynamic chord, v_x and v_z are the components of hull speed in wind-axis reference frame, α is the angle of attack, C_{L0} and C_{m0} are the coefficients of lift and pitching moment at $\alpha = 0$ with high lift devices deployed, $C_{L\alpha}$ and $C_{m\alpha}$ are the α-derivatives of lift and pitching moment .

A significant effect of the wing system is the pitch damping moment, which is related to pitch angular velocity and is introduced by means of the following expression:

$$\frac{\partial \mathbf{m}}{\partial \mathbf{q}} = \frac{\mathbf{1}}{\mathbf{4}} \cdot \boldsymbol{\rho_0} \cdot \mathbf{S} \cdot \mathbf{c^2} \cdot \mathbf{V} \cdot \mathbf{C_{mq}} \tag{4}$$

where C_{mq} is the pitching moment q-derivative and q is the dimensionless pitch angular velocity ($\dot{\vartheta}$), defined as follows:

$$\mathbf{q} = \dot{\vartheta} \cdot \frac{\mathbf{2c}}{\mathbf{V}} \tag{5}$$

Another important external force acting on the hull is the thrust provided by propellers, which is evaluated through the actuator disk model, by solving the following expression:

$$\frac{\mathbf{T^3}}{\mathbf{2} \cdot \mathbf{A} \cdot \boldsymbol{\rho_0}} + \boldsymbol{\eta_p} \cdot \mathbf{P} \cdot \mathbf{V} \cdot \mathbf{T} - (\boldsymbol{\eta_p} \cdot \mathbf{P})^{\mathbf{2}} = \mathbf{0} \tag{6}$$

where T is the thrust, P is the engine power, A is the propeller disk area and η_p is the propulsion efficiency. As Figure 7 shows, in the speed range of interest for the take-off run (0 - 25 m/s), thrust can be approximated as a linear function of the speed.

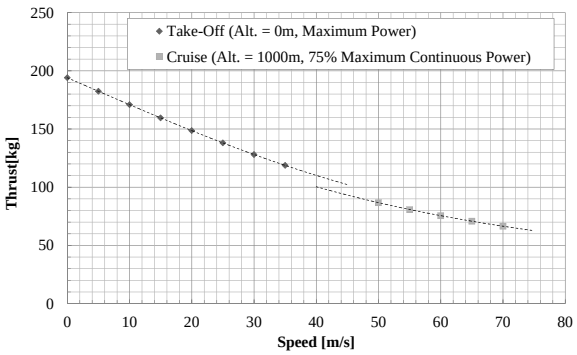

Figure 7. Actuator disk model: Thrust VS Speed

Finally, gravity is applied to the aircraft, for which mass, CG position and moments of inertia are defined.

4.2. Domain mesh

The system studied is symmetric with respect to xz plane in order to reduce the computational cost.

The domain mesh adopted is unstructured and composed of hexahedral elements, whose dimensions are refined in proximity of the hull surface, where eight

This is a pre-print version of:
Frediani, A., Cipolla, V., Oliviero, F. et al. A new ultralight amphibious PrandtlPlane: preliminary CFD design of the hull. Aerotec. Missili Spaz. 92, 77 - 86 (2013). https://doi.org/10.1007/BF03404665

layers of prismatic cells are extruded in order to enhance the alignment with the local flow direction.

In order to improve the grid resolution around the free surface, volumetric blocks with increasing anisotropic refinements, higher along the normal direction to the initial free surface plane, have been created. Further refinement blocks have been added in the regions close to the step section, in order to have a finer representation of the separated flow after the step.

As a result, CFD analyses have been performed by using a mesh of about 2.5×10^6 elements and choosing a time step $\Delta T = 10^{-3}$ seconds in order to reduce the local Courant Cu number, which is defined as follows:

$$\mathbf{Cu} = \mathbf{V} \cdot \frac{\mathbf{\Delta T}}{\mathbf{\Delta X}} \tag{7}$$

where ΔX is the length of the grid element along local speed (V) direction.

4.3. Time step

Time integration has been carried out using an implicit unsteady solver with a first order temporal scheme, while time steps of 10, 5 and 1 milliseconds have been considered [11].

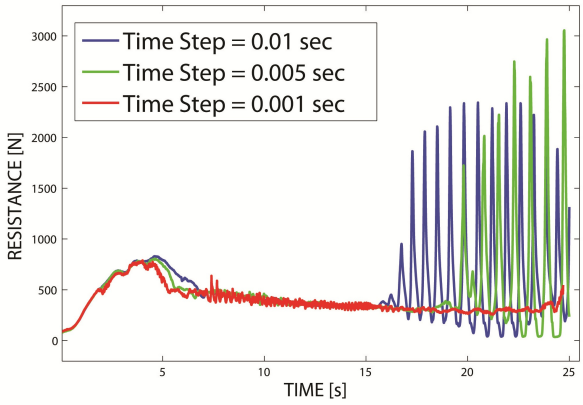

Figure 8. Effects of integration time steps [11]

The solutions obtained for the three different time step values, shown in Figure 8, have a common initial behaviour before the hump, after which some small differences can be observed. As the simulation time increases, such differences are bigger and the cases with longer time step (5 ms and 10 ms) present big oscillations.

One more example of 10 ms time step result is given in Figure 9, where unexpected vertical oscillations occur during planing phase, when speed is increasing and

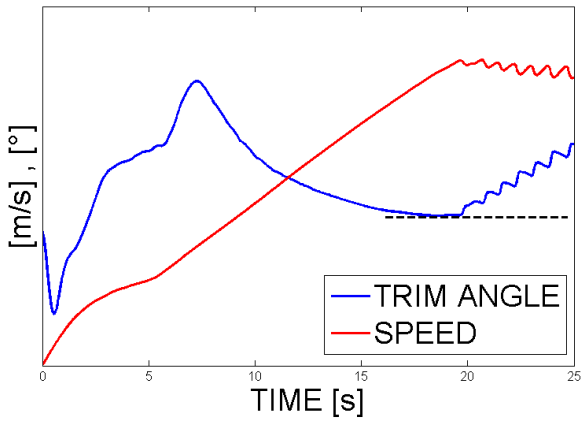

Figure 9. Oscillations in pitch angle and hull speed [11]

pitch angle is reducing. These oscillations are coupled with quick increase of pitch angle and resistance, which can reach high values. Therefore, aircraft acceleration is reduced and take-off speed can not be reached.

Such oscillations depend on the numerical scheme adopted in time integration; in fact, for of the cases observed, when reducing the time step from 10 ms to 5 ms, the hull's dynamics does not change, but the oscillations described before disappear or are delayed so that the take-off speed can be reached.

Finally, in some cases a time step of 5 ms is still too long and a value of 1 ms is needed; in these cases the oscillatory motion almost disappears, as Figure 8 shows.

5. Parametric analysis

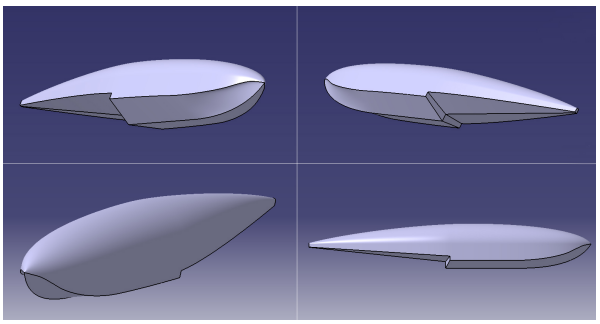

Figure 10. Reference hull

The parametric analyses has started from a reference hull, shown in Figure 10. The part of the body

This is a pre-print version of:
Frediani, A., Cipolla, V., Oliviero, F. et al. A new ultralight amphibious PrandtlPlane: preliminary CFD design of the hull. Aerotec. Missili Spaz. 92, 77 - 86 (2013). https://doi.org/10.1007/BF03404665

above chines is a simplified version of the actual fuselage, introduced to reduce modelling and computational time. The main dimensions of the reference hull are:

- length: 7000 mm;
- step depth: 150 mm;
- maximum beam at chines: 1200 mm;
- angle of afterbody keel: 6°;
- step distance from the bow: 3500 mm;
- CG distance from the bow: 3150 m;
- dead-rise angle at step section: 18°.

Starting from this configuration, 12 hull versions have been generated and analysed at take-off conditions.

The following design parameters have been varied with the aim of investigating their influence on the take-off run:

- planing-tail;
- step depth;
- planform angle of step;
- keel pad/spray rails presence (Figure 11);
- distance between CG and step section.

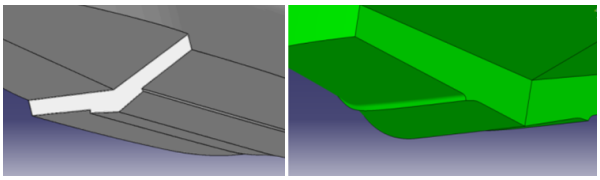

Figure 11. Keel pad (left) and spray rails (right)

In addition, an investigation of the angle of impact effects on accelerations experienced by occupants in case of emergency sea-landing has been carried out.

5.1. Effects of planing-tail

CFD simulations confirm that during take-off, a planing-tail hull may have lower resistance than conventional ones.

As can be observed in Figure 12, the planing-tail shows a lower resistance during the displacement phase, but also higher pitch angles during the whole run, which may cause a significant reduction in visibility during the take-off manoeuvre.

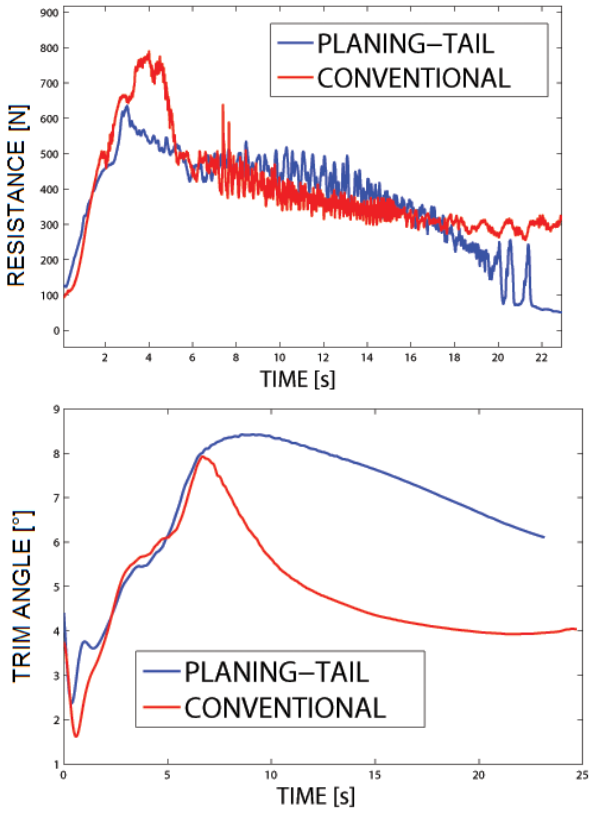

Figure 12. Comparison between planing-tail and conventional hulls [11]

Since safety is one of the main requirement for ultralight aircraft design and safety depends also on visibility, a conventional hull has been preferred to a planing-tail one.

Because of the good performance in terms of resistance, the planing-tail configuration could be applied to bigger aircraft, which are provided with more sophisticated avionic instruments.

5.2. Effects of step depth

The effect of step depth is described in Figure 13. A deeper step causes a reduction of the resistance hump, which is also anticipated; this positive effect is due to a more effective separation between water and hull. On the other side, a deeper step reduces the aerodynamic efficiency during flight; thus, a compromise solution has to be defined, in order to find the minimum step depth which allows to perform the take-off run.

5.3. Effects of planform angle

The effect of step planform angle is shown in Figure 14: a value of 10° represents a good compromise between easy manufacturing and good performances.

This is a pre-print version of:
Frediani, A., Cipolla, V., Oliviero, F. et al. A new ultralight amphibious PrandtlPlane: preliminary CFD design of the hull. Aerotec. Missili Spaz. 92, 77 - 86 (2013). https://doi.org/10.1007/BF03404665

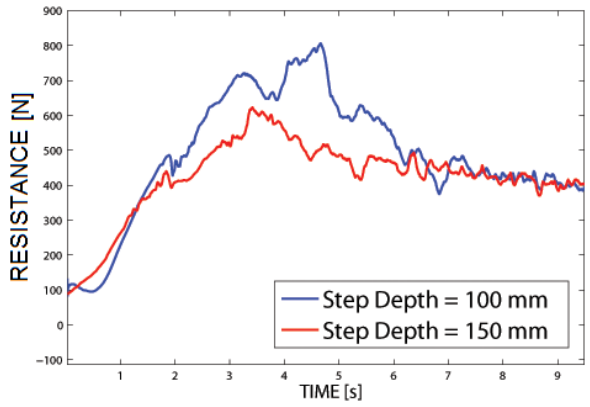

Figure 13. Effect of step depth on resistance [11]

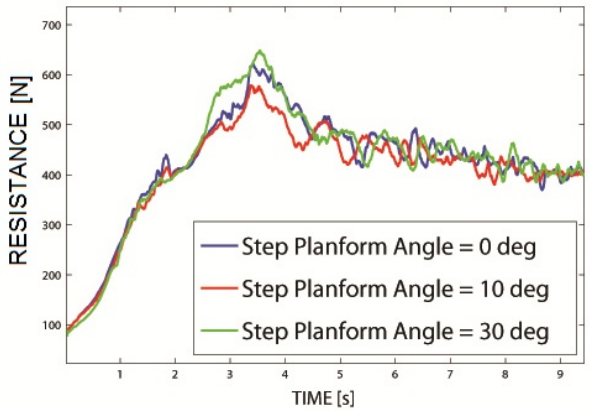

Figure 14. Effect of step planform angle on resistance [11]

5.4. Effects of keel pad and spray rails

As observed in [11], during planing phase, keel pad and spray rails have the positive effect of reducing the wetted area width, which means less resistance and lower pitch angles, providing better visibility to pilots.

5.5. Effects of distance between CG and step section

The effects of longitudinal distance between step and CG (ΔX) can be observed in Figure 15: the lowest value provides lower pitch angles but also a higher resistance and a higher level of oscillations, while the highest value is more stable shows a reduction of resistance but requires higher pitch angles at hump. An intermediate ΔX value gives the best compromise between performance and stability.

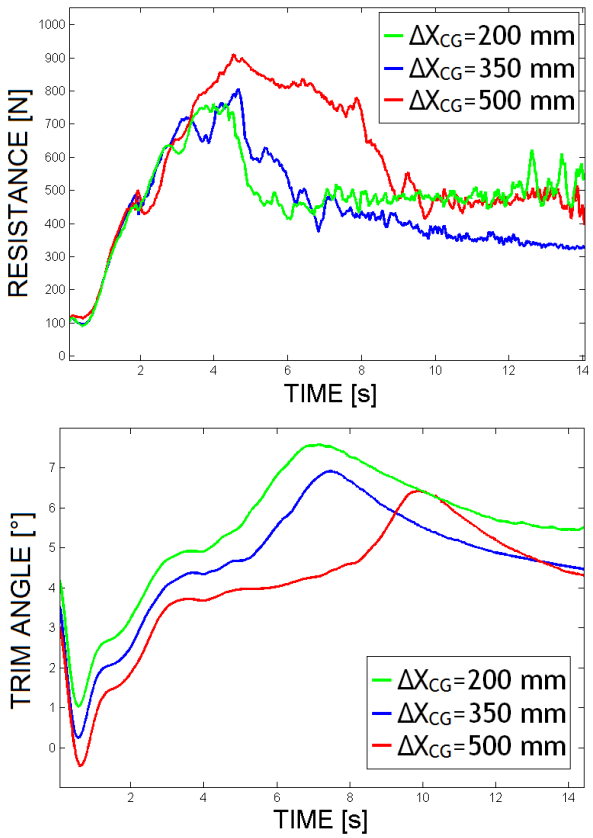

Figure 15. Effect of CG-step distance on resistance and pitch angle [11]

5.6. Effects of the angle of impact on accelerations experienced during emergency sea-landing

In the case of an emergency sea-landing, the Italian regulation requires that the occupants must be protected from shock due to impact, which implies that accelerations must be limited in term of magnitude (n_z) and duration (Δt).

It has been supposed that the impact on water occurs with ballistic parachute deployed a the maximum sink speed allowed, which, according to DULV (German Ultralight Association), is 7.5 m/s.

Such vertical speed value has been used to initialize the CFD simulations, in which the starting condition is the instant of impact on water.

Assuming that hull surfaces are infinitely rigid, different pitch angles have been simulated and the time response of vertical acceleration have been estimated.

As explained in details in [12], CFD runs have been performed adopting domain dimensions, time step values and mesh size resulting from sensitivity analyses carried out previously. Such characteristics are:

- time step of 2.5×10^{-3} seconds;

This is a pre-print version of:
Frediani, A., Cipolla, V., Oliviero, F. et al. A new ultralight amphibious PrandtlPlane: preliminary CFD design of the hull. Aerotec. Missili Spaz. 92, 77 - 86 (2013). `https://doi.org/10.1007/BF03404665`

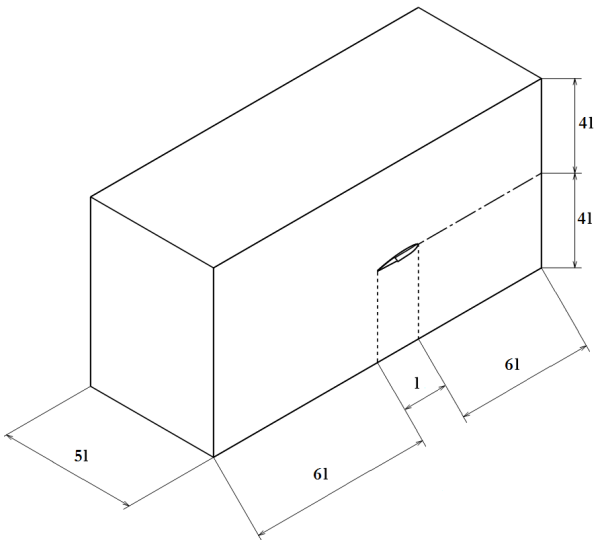

Figure 16. Dimensions of the domain adopted for sea-landing analyses [12]

- domain dimensions as shown in Figure 16, where l is the hull's length;
- 1.2×10^6 mesh elements.

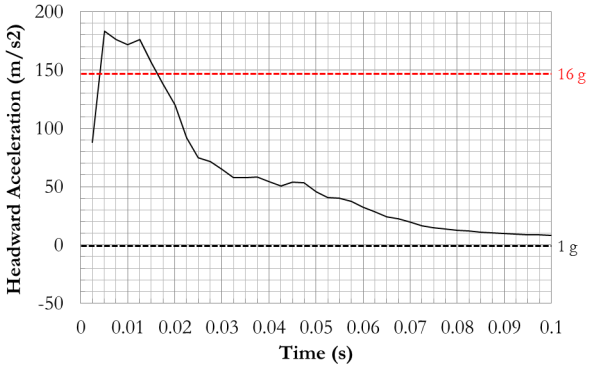

Figure 17. Emergency sea-landing at $\theta = 0°$: vertical acceleration vs. time [12]

Figure 17 shows one of the charts obtained from CFD analyses, which have been analysed to obtain the n_z - Δt combinations reported in Table 2, where θ is the angle of impact, positive for nose-up rotations, and n_z is the vertical load factor, defined as follows:

$$\mathbf{n_z = 1 + \frac{a_z}{g}}, \tag{8}$$

in which a_z is the vertical acceleration and g is the gravitational acceleration.

Table 2
Results of emergency sea-landing simulations [12]

θ [deg]	n_z max. [g]	Δt [s]	Level of Injuries
+5	20.0	0.005	Moderate
0	18.0	0.010	Moderate
-4	10.0	0.015	Uninjured
-6	8.5	0.025	Uninjured
-8	7.0	0.040	Uninjured

The level of injuries indicated in Table 2 has been defined according to [13], in which it is demonstrated that the human body can undergo vertical accelerations without injuries when the exposure time is lower than 0.04 s and the load factor is lower than 16 g.

As shown in Table 2, even though exposure time is not longer than 0.04 s, positive or null angles of impact make the amphibian undergo accelerations that can injury the occupants. For negative angles, instead, acceleration peaks are lower than 16 g and, then, injuries are not probable.

6. Results

The results of the parametric analysis have been used to define design guidelines and select some hull configurations for towing tank tests which have been carried out at the CNR-INSEAN in Rome.

In addition, performance data of such configurations have been used for scaled models design.

6.1. Selected hull configurations

The two selected configurations are shown Figure 18, in which it can be observed that the hulls differ only for the step position. Both "T700" hull and "T400" one have the following characteristics:

- conventional hull, instead of planing-tail;
- step depth = 150 mm ;
- step planform angle = 10°;
- presence of a keel pad;
- CG-step distance of 350 mm for the "T700" and 50 mm for the "T400".

The take-off performance data of "T400" and "T700" hulls, listed in Table 3, show that the "T700" have a better behaviour at the hump, requiring lower speed and pitch angle to perform the transition from the displacement phase to the planing one, while the

This is a pre-print version of:
Frediani, A., Cipolla, V., Oliviero, F. et al. A new ultralight amphibious PrandtlPlane: preliminary CFD design of the hull. Aerotec. Missili Spaz. 92, 77 - 86 (2013). https://doi.org/10.1007/BF03404665

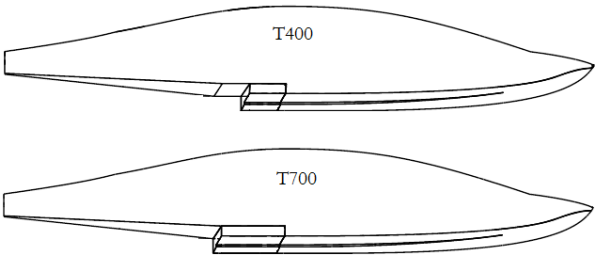

Figure 18. Hull shapes selected for towing tank tests

"T400" have a more stable planing phase, with smaller pitch angle oscillations (Figure 19).

Table 3
"T400" and "T700" hulls: take-off run performance (CFD)

Performance	T700	T400
Take-off Speed [m/s]	29	29
Hump Speed [m/s]	9	11
Hump Resistance [kg]	95	95
Hump Pitch Angle [deg]	8	8.5

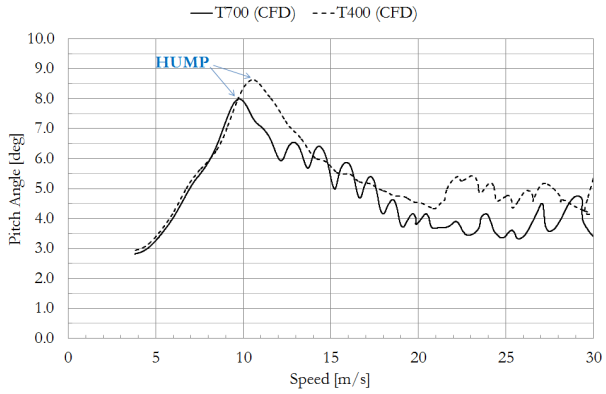

Figure 19. CFD results on "T400" and "T700" hulls: Pitch Angle vs. Speed

6.2. Design of scaled models

CFD data have been used for one of the most important design parameter of the test model: the scale factor λ, defined as the ratio between a reference length of the full-scale amphibian (l) and the same dimension of the model (l_m):

$$\lambda = \frac{\mathbf{l}}{\mathbf{l_m}} \quad . \tag{9}$$

The general purpose of the towing tank tests is to measure the loads applied from water to the hull, while this latter undergoes additional forces coming from the test rig and representing the effects of wings, control surfaces and propellers. The hull model and the test rig are shown in Figure 20.

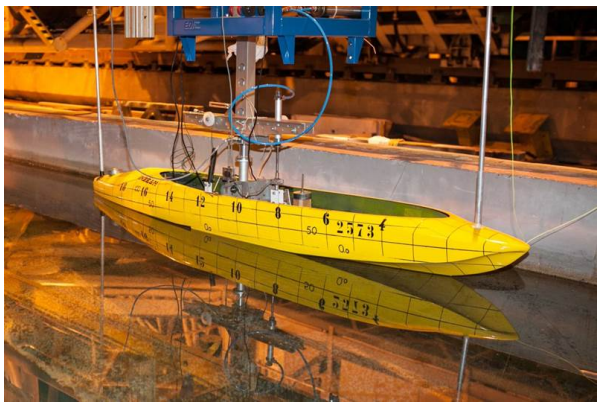

Figure 20. Hull model and test rig at the towing tank facility of CNR-INSEAN (Rome)

Since measures are performed on water loads, a hydrodynamic similitude criterion has been applied requiring that the Froude number is the same for both the amphibian and the scaled model. Given the following Froude number definition:

$$\mathbf{Fr} = \frac{\mathbf{V}}{\sqrt{\mathbf{g} \cdot \mathbf{l}}} \quad , \tag{10}$$

where V is the hull speed and l is a reference length, the model speed V_m can be calculated as follows:

$$\mathbf{V} = \mathbf{V_m} \cdot \sqrt{\lambda} \quad . \tag{11}$$

It is worth of notice that for safety reason, the maximum test speed of the towing tank facility is limited to 15 m/s, therefore the choice of λ has a strong influence on the maximum speed that can be represented.

In addition, a second criterion has been introduced to scale the model mass by requiring that the equilibrium condition between weight and lift is obtained at the same lift coefficient (C_L), which is defined as follows:

$$\mathbf{C_L} = \frac{\mathbf{L}}{\frac{\mathbf{1}}{\mathbf{2}} \cdot \rho \cdot \mathbf{S} \cdot \mathbf{V^2}} \quad , \tag{12}$$

This is a pre-print version of:
Frediani, A., Cipolla, V., Oliviero, F. et al. A new ultralight amphibious PrandtlPlane: preliminary CFD design of the hull. Aerotec. Missili Spaz. 92, 77 - 86 (2013). https://doi.org/10.1007/BF03404665

where L is the lift, ρ is the air density and S is a reference area of the amphibian.

Observing that the reference area of the model (S_m) is given by

$$\mathbf{S_m} = \frac{\mathbf{S}}{\boldsymbol{\lambda^2}} \quad , \tag{13}$$

given the equilibrium condition $L = M \cdot g$ and standing Equation 11, the following expression relates the model mass (M_m) to the amphibian mass (M):

$$\mathbf{M_m} = \frac{\mathbf{M}}{\boldsymbol{\lambda^3}} \quad . \tag{14}$$

According to CFD results, towing tank test should represent the maximum speed of 29 m/s, which is the estimated take-off speed. Given the 15 m/s limitation of the towing tank facility, from Equation 11 a minimum λ value of 4 can be found.

Such value is not feasible, since it is not possible, or at least very difficult, to meet the mass requirement, building a testing system (model + test rig) which is as light as 9 kg, as prescribed from Table 4.

Table 4
Effects of scale factor on test model speed and mass

λ	V [m/s]	V reduced [m/s]	M [kg]
1	29.0	25.0	584
λ	V_m [m/s]	V_m reduced [m/s]	M_m [kg]
2	20.5	17.7	73
3	16.7	14.4	22
4	14.5	12.5	9
5	13.0	11.2	5

Therefore, the scale factor has been defined as a compromise between the minimum system mass and the maximum speed represented.

Table 4 shows that reducing the reference speed up to 25 m/s, which allows to represent about the 70% of the total take-off run, a λ value of 3 can be selected.

7. Conclusions

CFD analyses have been performed on the hull of a ultralight amphibious PrandtlPlane by means of the software STAR-CCM+ by CD-Adapco, in order to study the effects of design parameters on take-off performance and define the hull configurations to be studied in a following towing tank test campaign.

Taking Italian regulation into account, different hull configurations have been modelled and analysed in order to achieve a good compromise between performance, stability and safety, for which pilot visibility and accelerations in case emergency sea-landing have been taken into account.

As a result, two hull shapes have been selected for the towing tank tests. The two configurations have the same design parameters with the only exception of the distance between the center of gravity and the step section, which influences the transition from the displacement phase to the plaining one and the dynamic stability during this latter.

The resulting hull configurations and performance data have been used for the design of scaled models and, in particular, to define a scale factor. Given similitude criteria, CFD prediction of take-off speed, test facility and manufacturing constraints, a scale factor of 3 has been chosen.

REFERENCES

1. A. Frediani, "The Prandtl wing", Von Karman Institute, Lecture series on Innovative Configuration and Advanced Concepts for Future Civil Aircraft, 2005.
2. L. Prandtl, "Induced drag of multiplanes", *NACA Technical Note*, no. 182, 1924.
3. A. Frediani, E. Rizzo, V. Cipolla, L. Chiavacci, C. Bottoni, J. Scanu and G. Iezzi, "Optimization methods for ULM PrandtlPlane design and preliminary flight tests on scaled models", *CEAS 2008*, pp. 685–713, London, 2008.
4. D. Savitsky, "Hydrodynamic Design of Planing Hulls", *Marine Technology*, Vol. 1, No. 1, pp. 71–95, 1964.
5. J. R. Dawson, R. C. Walter and E. S. Hat, "Tank test to determine the effect of varying design parameters of planing-tail hulls I - effect of varying length, width and plan-form taper of afterbody", *NACA Technical Note*, No. 1062, Langley Memorial Aeronautical Laboratory, 1946.
6. C. C. Yates and J. M. Riebe, "Aerodynamic characteristics of three planing-tail flying-boat hulls", *NACA Technical Note*, No. 1306, Langley Memorial Aeronautical Laboratory, 1947.
7. R. McKann and H. B. Suydam, "Hydrodynamic characteristics of an aerodynamically refined planing-tail hull", *NACA Research Memorandum*, No. L8G16, Langley Memorial Aeronautical Laboratory, 1948.
8. Decreto del Presidente della Repubblica n. 133, 9/7/2010. Nuovo regolamento di attuazione della Legge 106/1985 concernente la Disciplina del volo da diporto o sportivo. (G.U. n. 193 del 19/8/2010 - Suppl. Ordinario n.197)
9. Ministero delle Infrastrutture e dei Traasporti, Decreto 22/11/2010. Caratteristiche degli apparecchi per il volo da diporto o sportivo di cui all'allegato tecnico alla legge 25 marzo 1985, n. 106. (G.U. n. 287, 9/12/2010)
10. V. Cipolla, E. Rizzo, "Progetto IDINTOS: attività di progettazione e consulenza nello sviluppo di un velivolo anfibio ultraleggero PrandtlPlane", *Technical Report*, SkyBox Engineering Srl, Pisa 2012.
11. M. Lucchesi and T. Lippi, "Progetto concettuale e analisi CFD di uno scafo per anfibio PrandtlPlane ultraleggero", *M.Sc. Thesis*, Department of Aerospace Engineering, University of Pisa, Italy, 2011.
12. S. Luci ,"Utilizzo del codice STAR-CCM+ nello studio delle manovre di decollo ed atterraggio di un idrovolante ultraleggero Prandtlplane", *M.Sc. Thesis*, Department of Aerospace Engineering, University of Pisa, Italy, 2011.
13. A. M. Eiband, "Human Tolerance to Rapidly Applied Accelerations: A Survey of the Literature", *NASA Memo*, No. 5-19-59E. Washington, 1959.

This is a pre-print version of:
Frediani, A., Cipolla, V., Oliviero, F. et al. A new ultralight amphibious PrandtlPlane: preliminary CFD design of the hull. Aerotec. Missili Spaz. 92, 77 - 86 (2013). https://doi.org/10.1007/BF03404665